AFAPL-TR-79-2059
VOL. 1

LEVEL II (2)

INVESTIGATION OF THE PRODUCTION OF HIGH DENSITY UNIFORM PLASMAS

D.H.DOUGLAS-HAMILTON AND P.ROSTLER

AVCO EVERETT RESEARCH LABORATORY, INC.
2385 REVERE BEACH PARKWAY
EVERETT, MA 02149

MAY 1979

FINAL REPORT FOR PERIOD 2 April 78 - 2 April 79

Approved for public release; distribution unlimited

AIR FORCE AERO PROPULSION LABORATORY
AIR FORCE WRIGHT AERONAUTICAL LABORATORIES
AIR FORCE SYSTEMS COMMAND
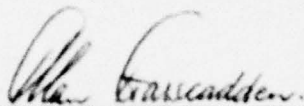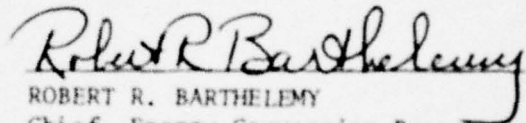WRIGHT-PATTERSON AIR FORCE BASE, OHIO 45433
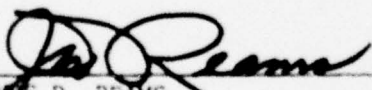
79 14 11 087

ALAN GARSCADDEN
Research Physicist

ROBERT R. BARTHELEMY
Chief, Energy Conversion Branch

FOR THE COMMANDER

JAMES D. REAMS
Chief, Aerospace Power Division

REPORT DOCUMENTATION PAGE	READ INSTRUCTIONS BEFORE COMPLETING FORM

1. REPORT NUMBER	2. GOVT ACCESSION NO.	3. RECIPIENT'S CATALOG NUMBER
AFAPL-TR-79-2059 Vol. I		

4. TITLE (and Subtitle)

INVESTIGATION OF THE PRODUCTION OF HIGH DENSITY UNIFORM PLASMAS. Volume I.

5. TYPE OF REPORT & PERIOD COVERED

Final Report,
2 April 78 — 2 April 79

6. PERFORMING ORG. REPORT NUMBER

7. AUTHOR(s)

D.H. Douglas-Hamilton and P. Rostler

8. CONTRACT OR GRANT NUMBER(s)

F33615-78-C-2013

9. PERFORMING ORGANIZATION NAME AND ADDRESS

Avco Everett Research Laboratory, Inc.
2385 Revere Beach Parkway
Everett, Massachusetts 02149

10. PROGRAM ELEMENT, PROJECT, TASK AREA & WORK UNIT NUMBERS

2308 55 02

11. CONTROLLING OFFICE NAME AND ADDRESS

Air Force Aero Propulsion Laboratory
Air Force Systems Command, U.S. Air Force
Wright Patterson A.F.B. 45433

12. REPORT DATE

May 1979

13. NUMBER OF PAGES

43

14. MONITORING AGENCY NAME & ADDRESS(if different from Controlling Office)

15. SECURITY CLASS. (of this report)

Unclassified

15a. DECLASSIFICATION/DOWNGRADING SCHEDULE

16. DISTRIBUTION STATEMENT (of this Report)

Approved for public release; distribution unlimited

17. DISTRIBUTION STATEMENT (of the abstract entered in Block 20, if different from Report)

18. SUPPLEMENTARY NOTES

19. KEY WORDS (Continue on reverse side if necessary and identify by block number)

Electron Beam Discharge
Streamers
Discharge Stability
Laser

20. ABSTRACT (Continue on reverse side if necessary and identify by block number)

The discharge streamer instability, which leads to arcing in non-self-sustaining discharges is investigated experimentally and theoretically. Framing camera studies of streamer growth from the cathode of an e-beam sustained discharge in various gases under various discharge conditions are described, analyzed, and compared with theoretical predictions. A previously developed ⟶ next page

DD FORM 1473 EDITION OF 1 NOV 65 IS OBSOLETE
1 JAN 73

048450

(20)

Cont.

model of the streamer is extended to include a more detailed
description of the density, temperature, and input power dis-
tributions around the streamer tip. —> to page 1

FOREWORD

This work was performed at Avco Everett Research Laboratory, Inc., under contract number F33615-78-C-2013. The present report is the first of two volumes.

iii

TABLE OF CONTENTS

LIST OF ILLUSTRATIONS

SECTION I

INTRODUCTION

cont.

Stable high-density plasma discharges have many applications in plasma physics. An especially significant example is the use of these discharges in high-power gas lasers. The work described here concerns investigation of the external ionization e-beam sustainer method of producing a high-density discharge, together with the advantages and instabilities peculiar to that system.

The high-pressure electron beam stabilized (EBS) discharge exists stably in two regimes, distinguished by their modes of electron production and loss. First, if secondary ionization is much less than EB ionization (i.e., if $S \gg A_1 V_e n_e$ where S is the ionization source function, A_1 is the first Townsend coefficient, n_e is electron number density and V_e is electron drift velocity), we have the conventional EBS discharge, in which electron production is balanced by electron-neutral attachment, by electron-positive ion recombination, or in general by a combination of both. Second, if $S \ll A_1 V_e n_e$ we have the so-called avalanche mode; the EB acts as a trigger, and the number density of electrons increases until the number lost by recombination equals the number gained by Townsend multiplication. We note that in gases exhibiting electron attachment, there is a third mode of discharge operation in which negative and positive ion current is much greater than electron current. In the work described here, the discharge operates in the first mode, and recombination processes dominate the electron losses.

1. ATTACHMENT INSTABILITIES

Attachment instabilities, discovered and investigated under this program,[1,2] occur when the differential gas conductivity becomes negative due to enhanced electron attachment by neutral molecules at higher electric fields, and are significant at high fields and low pressures in many gases. Thermal and acoustic instabilities[3] occur generally for discharges, providing limits on the total energy that can be introduced into the discharge. As pointed out by Nighan and Wiegand,[4] vibrational instabilities exist when significant energy is stored in molecular vibrational modes; increase in gas temperature accelerates the collisional transformation of this energy to translational, resulting in runaway heating of the discharge medium.

1. Douglas-Hamilton, D.H., Mani, S.A., J. Appl. Phys. 45, 4406 (1974)

2. AFOSR Final Report, Contract F44620-70-C-0023 (1974).

3. Jacob, J.H. and Mani, S.A., Appl. Phys. Lett. 26, 53 (1975).

4. Nighan, W.L. and Wiegand, W.J., Appl. Phys. Lett. 25, 633 (1974).

2. STREAMERS

Both attachment and thermal-acoustic instabilities are large-scale positive column instabilities, and only the initial phases of their growth can be described by linear analysis. The secondary phases of all these instabilities appear to be the formation of discharge streamers*, and we are now beginning to obtain detailed information about this nonlinear phase of the discharge instability.

Streamers of this type in EBS discharges were first discovered at AERL under this program. Since that time, streamers have been found to occur quite commonly in such discharges, and, indeed, are responsible for arcing in many high power gas discharge lasers. Examples are shown in Figures 1 and 2. Accordingly, in recent work under this program, we have concentrated on study of the streamer phenomenon and have succeeded both in verifying the essential elements of our original model of a streamer, and in obtaining new, more detailed data about streamer propagation.

In our original model, shown in Figure 3, a streamer was described as a cylinder of hot and consequently conductive gas (both because of its lower density, and because of the thermal ionization of the gas at the equilibrium streamer temperature near 6000°K). This conducting cylinder protrudes into the discharge; near its head there will be both a strong field and a high current density (just as would occur near the tip of a wire protruding from the cathode). Both field and current act to raise the conductivity of gas beyond the tip - the field by ionization and the current by heating. The streamer grows across the discharge at a velocity determined by the time required to heat the gas up to conducting temperature. When it reaches the appropriate electrode, or joins with a streamer propagating from the opposite electrode, a low-impedance circuit is formed and an arc interrupts the discharge.

---

*Non self-sustaining discharge streamers must be distinguished from the electron-avalanche type of streamer appearing in spark breakdown. In the first case the streamer closely resembles an incomplete arc and photionization processes may be neglected, where in the second case photionization generates the seed electrons in the avalanche. In the present work we discuss only the non self-sustaining discharge streamer.
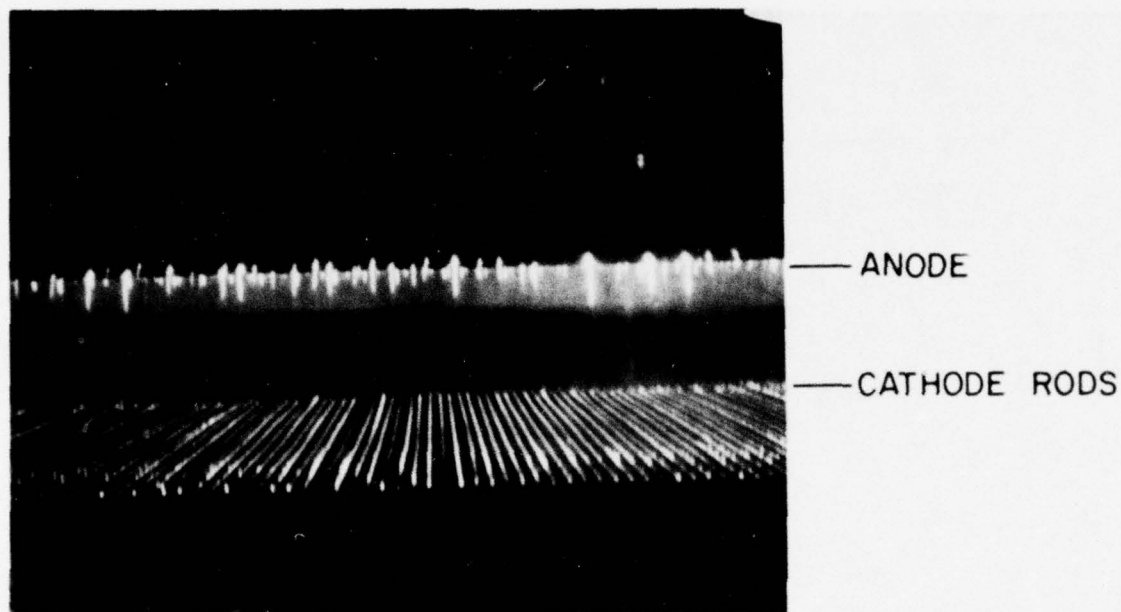
E1075

Figure 1   Pulsed Discharge Streamers. Electron density
            $\sim 3 \times 10^{12}$ cm-3, electric field 5000 V/cm,
            pressure 1 atm. Gas mixture $He:N_2:CO_2$; 3:2:1.
            Electron beam enters through cathode, at bottom.
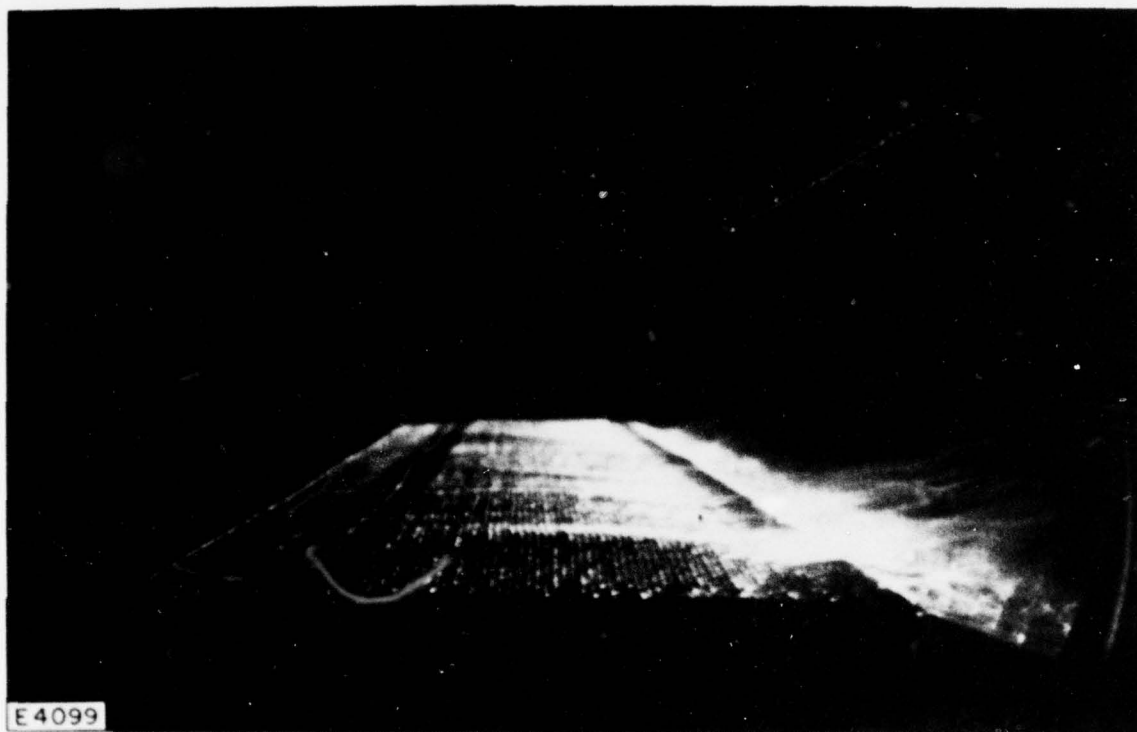
Figure 2   Flowing Discharge Streamers. Flow is from left to
            right: e-beam enters through cathode, at bottom.
            Pressure 380 torr, flow velocity Mach 0.4, electron
            density 3×10^{11} cm^{-3}, electric field 2.8 kV/atm cm,
            gas mixture He:N_2:CO_2; 16:8:1.

4

UPPER ELECTRODE
$V = V_2$

D

CAP SPHERE
$V = V_0$
RADIUS a

C

STREAMER CYLINDER
RADIUS b
LENGTH C

LOWER ELECTRODE
$V = 0$

G1977
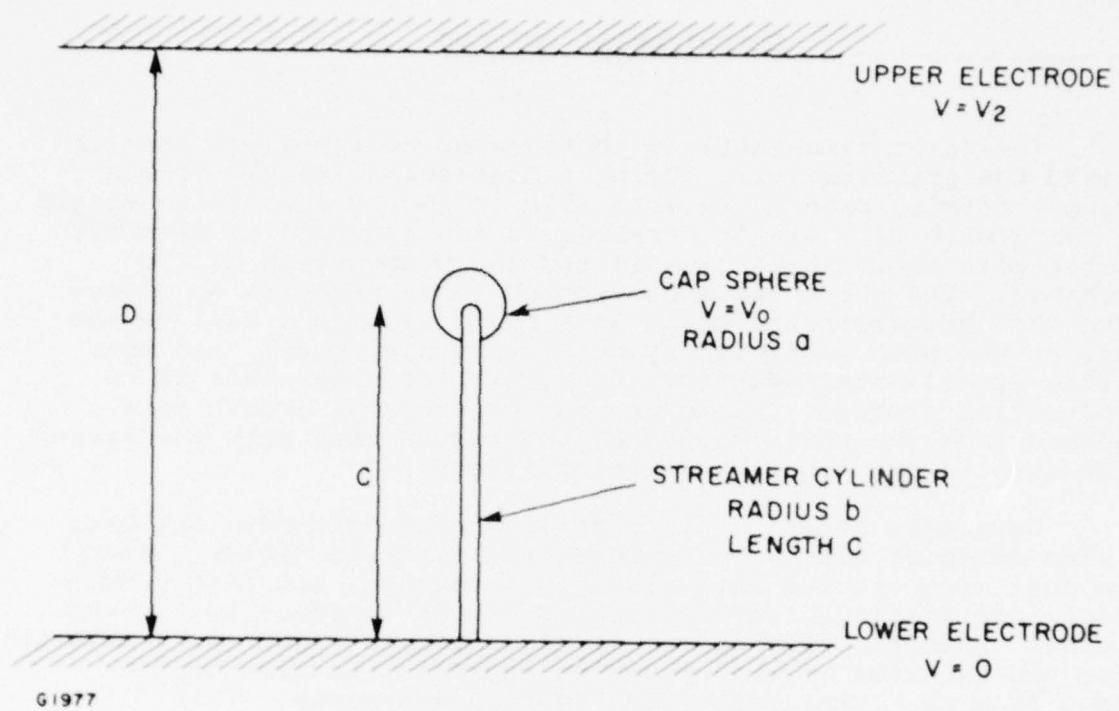
Figure 3　Model for Streamer Propagation

SECTION II

EXPERIMENTAL RESULTS

The first time-resolved photographs of streamers were obtained the previous year. Using a high-speed (44,000 frames/second) framing camera, we were able to record successive stages in the growth of a single streamer, which provided us with much better data about the structure and the propagation of the streamer. The photo sequences showed that streamers do indeed have the characteristic shape of a cylinder with a ball on the end, as had been predicted by our theoretical model, and that within experimental accuracy, the growth of a streamer is an exponential process. Moreover, the exponential growth rate deduced from the photo sequences correlates well with the arcing time seen in the discharge current traces.

Data were taken in nitrogen at atmospheric pressure over a wide range of discharge currents and electric fields. When the data were grouped into slow, intermediate, and fast growth cases, and displayed parametrically in the current-power plane, a clear dependence was apparent. As shown in Figure 4, a straight line can be drawn in this plane to separate the slow growth cases from the intermediate and fast growth cases. This "line of constant growth rate" corresponds to

$$P - 3.8 \, j = 1 \qquad (1)$$

where P is in kW/cm^3 and j is in A/cm^2. As can be seen from Figure 4, this line is quite precisely defined by our data over a considerable parametric range.

In the P-j plane, a straight line through the origin would represent a constant value of electric field. The observed instability line is almost, but not quite of this form. The difference is apparent when the data are plotted against electric field. This is done in Figure 5, where the same data points, and the same separation line are shown in the P-E plane. Here the line is a hyperbola. At large powers, the line is nearly vertical, implying that γ is there dependent primarily upon E. But at lower powers and higher electric fields, the line is nearly horizontal, indicating that γ is mainly P dependent in that region.

In the early work just described, the framing camera was focused on a small strip of the discharge extending from cathode to anode, and streamers were made to form there by attaching a

6

HI280
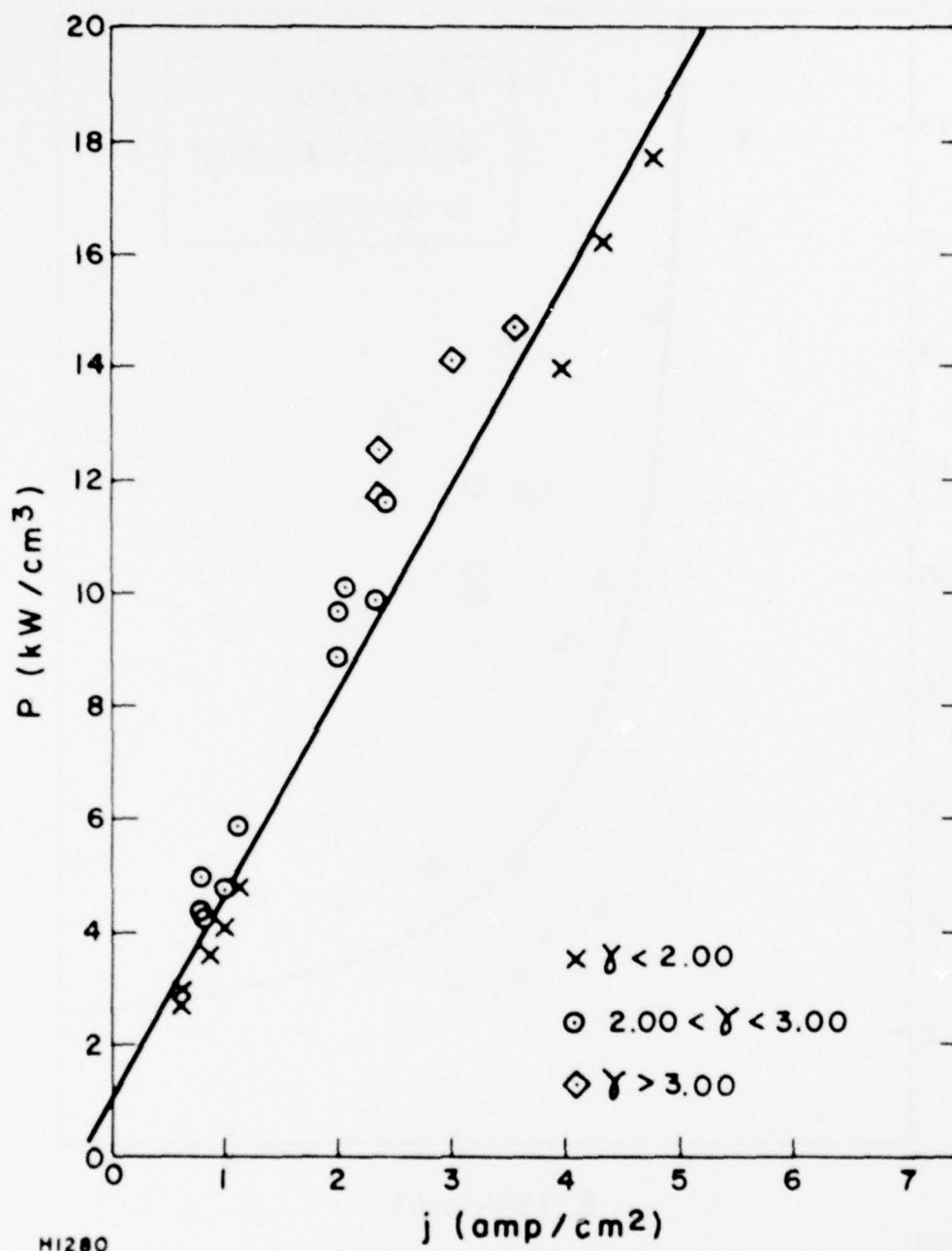
Figure 4   Dependence of Streamer Growth Rate Upon Discharge
            Power Density and Current Density. γ is in units
            of $(100 \ \mu s)^{-1}$.
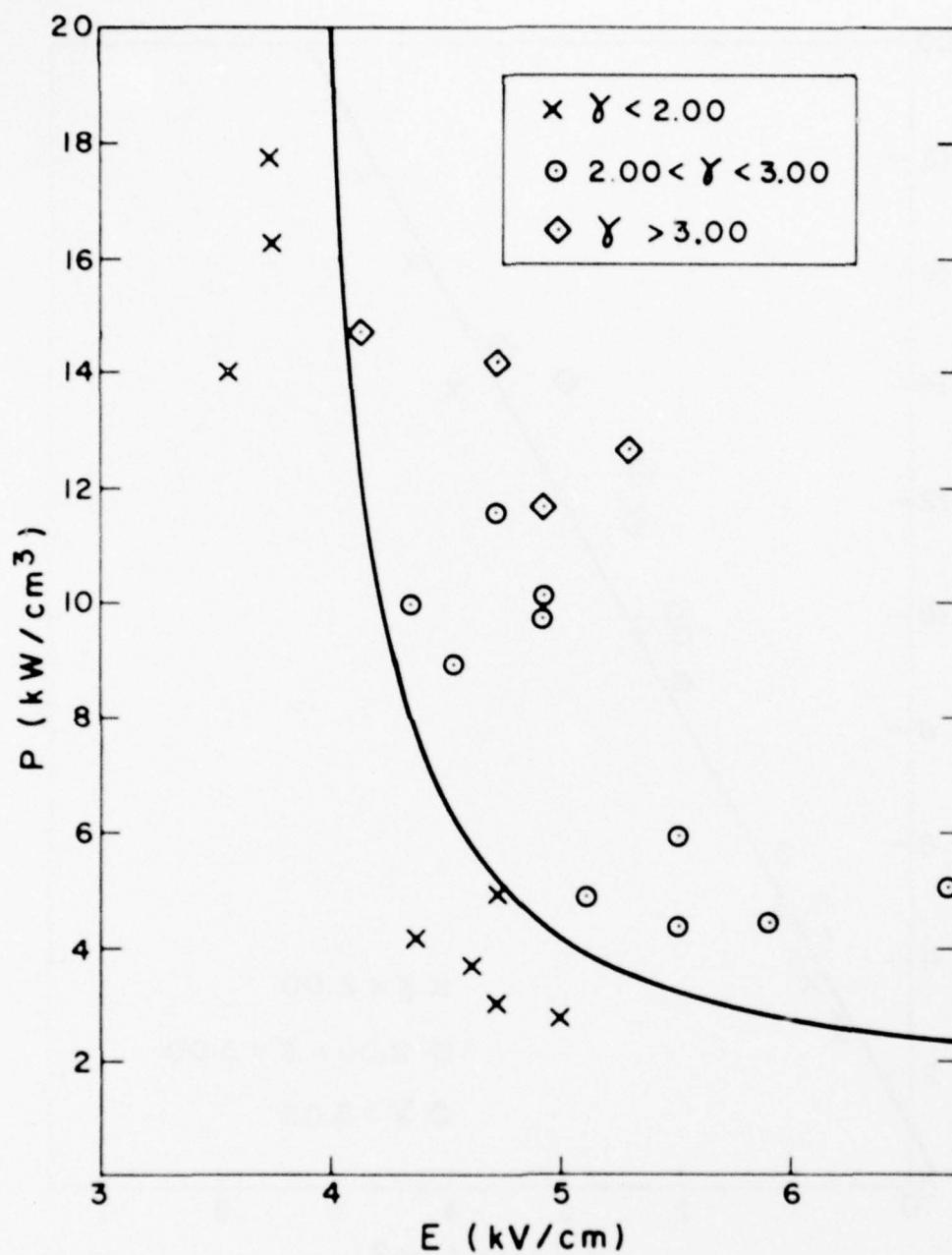
Figure 5   Dependence of Streamer Growth Rate Upon Discharge
Power Density and Electric Field. γ is in units
of $(100 \ \mu s)^{-1}$.

H1281

8

small loop of tungsten wire to the cathode. This forced the streamers to start with a size of about 1 mm and to always start at the same place, which made the data reproducible, permitting us to determine Eq. (1), but which prevented us from learning anything about streamer initiation, or comparing streamer growth at different points within the discharge.

During this past year, we improved our experimental apparatus and technique to the point where we could obtain clear and detailed framing camera photographs of the entire discharge. This enabled us to dispense with the tungsten wire and study spontaneous growth of streamers from a smooth, rounded cathode plate. The rebuilt apparatus is shown schematically in Figure 6. The actual device is shown in Figures 7a through 7d. It includes a completely new discharge cell which is cleaner, more convenient, and affords a much improved view of the discharge region. The cell contains a reflecting prism which gives a side view of the discharge through a window in the end plate of the cell. We also added to the cell a pair of coils and associated pulsing circuitry that can be used to impose an external magnetic field transverse to the discharge current. This field exerts a sideways force on the discharge, but for fields less than 200 G, this force should not have much effect on a uniform discharge in our apparatus. However, in a streamer the current density is orders of magnitude above the background level and our calculations suggested that the proportionally larger force might be significant. A sideways force would tend to push the streamer through the surrounding cold gas, which should help slow down its growth. Addition of the coils enabled us to determine whether fields compatible with e-beam propagation could have an observable effect on streamer growth.

In this year's experiments, the framing camera was run in half-frame mode (22,800 frames/second) to obtain a longer exposure and a larger field-of-view. A small resistance (5 Ω) was added in series with the discharge to reduce the brightness of the final arcs which had caused back-fogging of many of the framing camera sequences taken the previous year. These changes enabled us to obtain much better photographs of streamers.

Examples of the new data are shown in Figures 8 through 13 which show streamers in nitrogen discharges at various pressures, electric and magnetic fields, and power loading. Each frame of each sequence shows the entire width of the discharge and the field-of-view extends from the cathode to about two-thirds of the way to the anode. The cathode is at the bottom of each frame. (It can be seen in some after the arc.) The view is exactly across the face of the cathode. The framing rate is one frame every 44 μs and the exposure of each is 18 μs. The e-beam entered through the anode (a plate with a hexagonal pattern of holes) and the magnetic field, when present, is along the line-of-sight. The width of the cathode is 5 cm and the anode to cathode spacing is 1 in.

9

DISCHARGE CELL

H7574
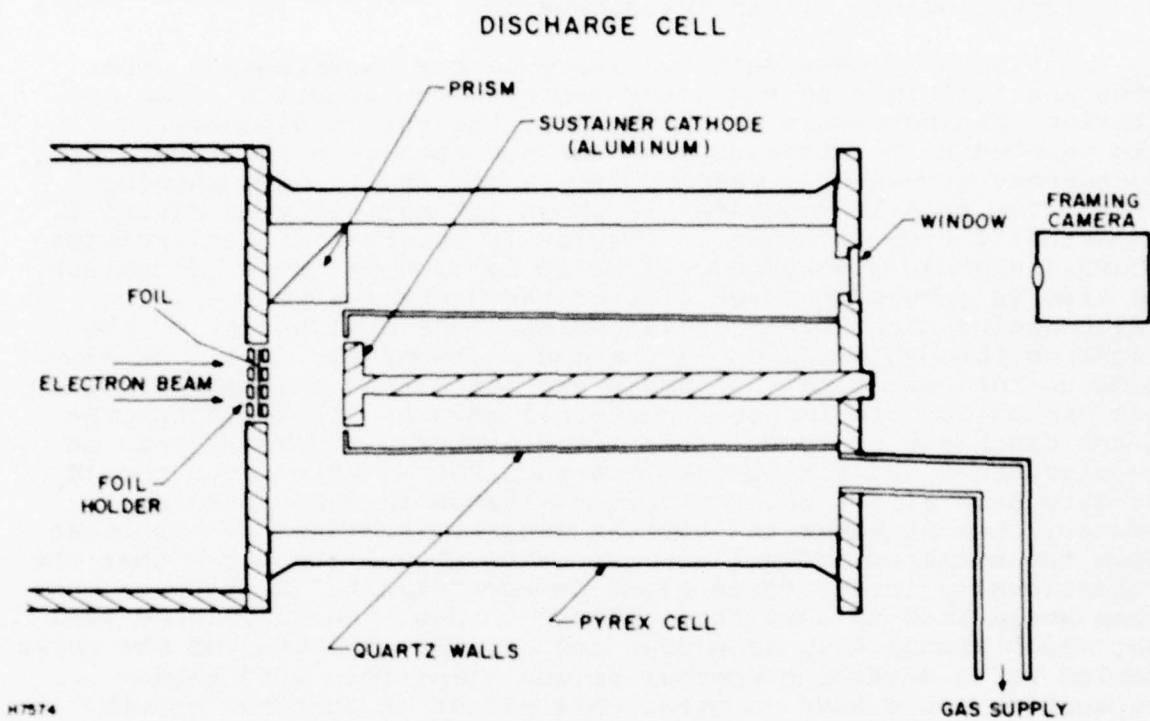
Figure 6   Schematic Diagram of EBS Facility
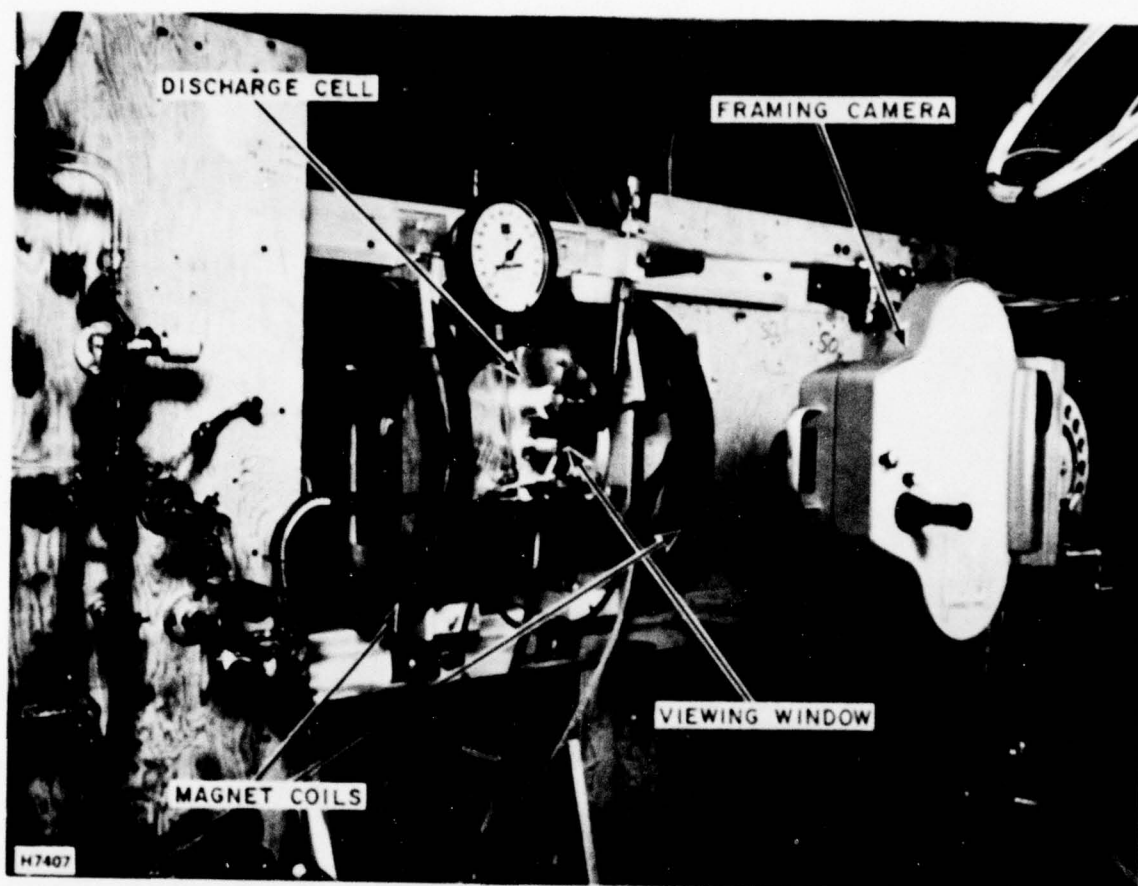
Figure 7a   The Rebuilt Mini-Bang Apparatus
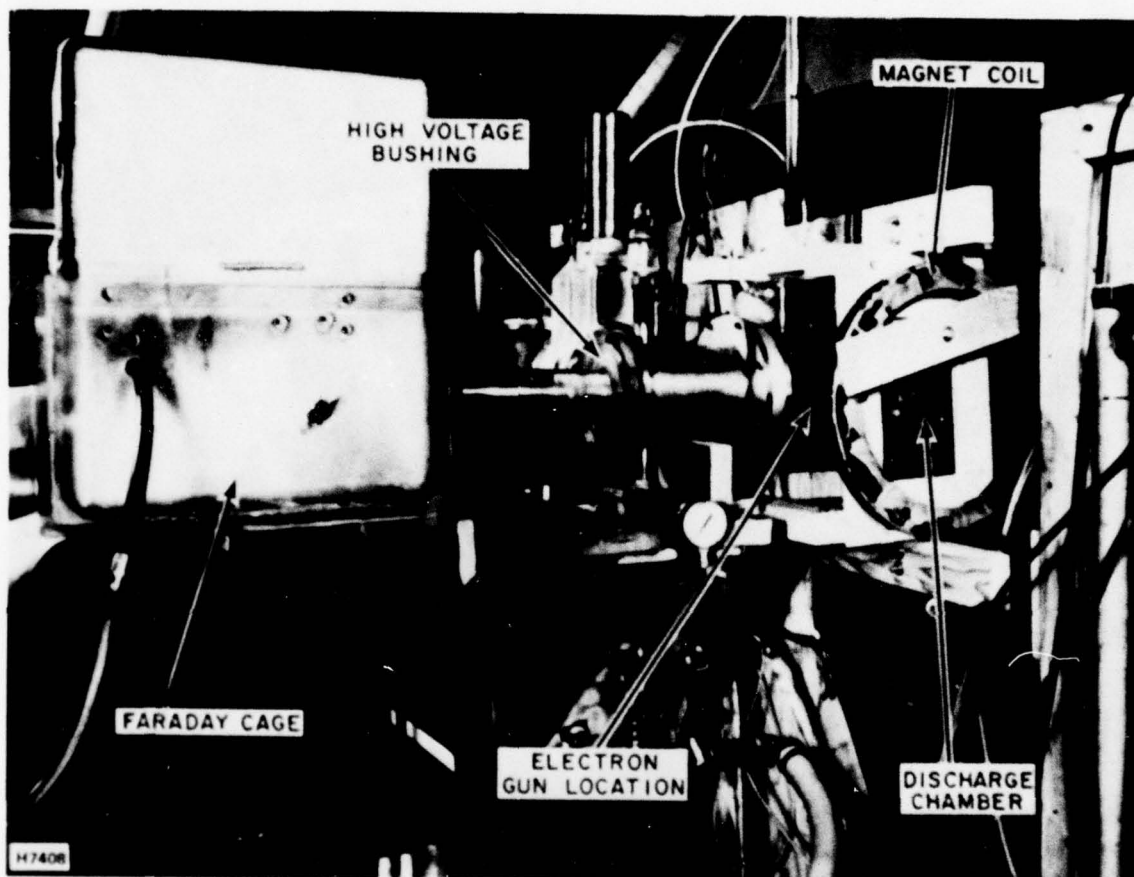
Figure 7b   Another View of the Rebuilt Apparatus
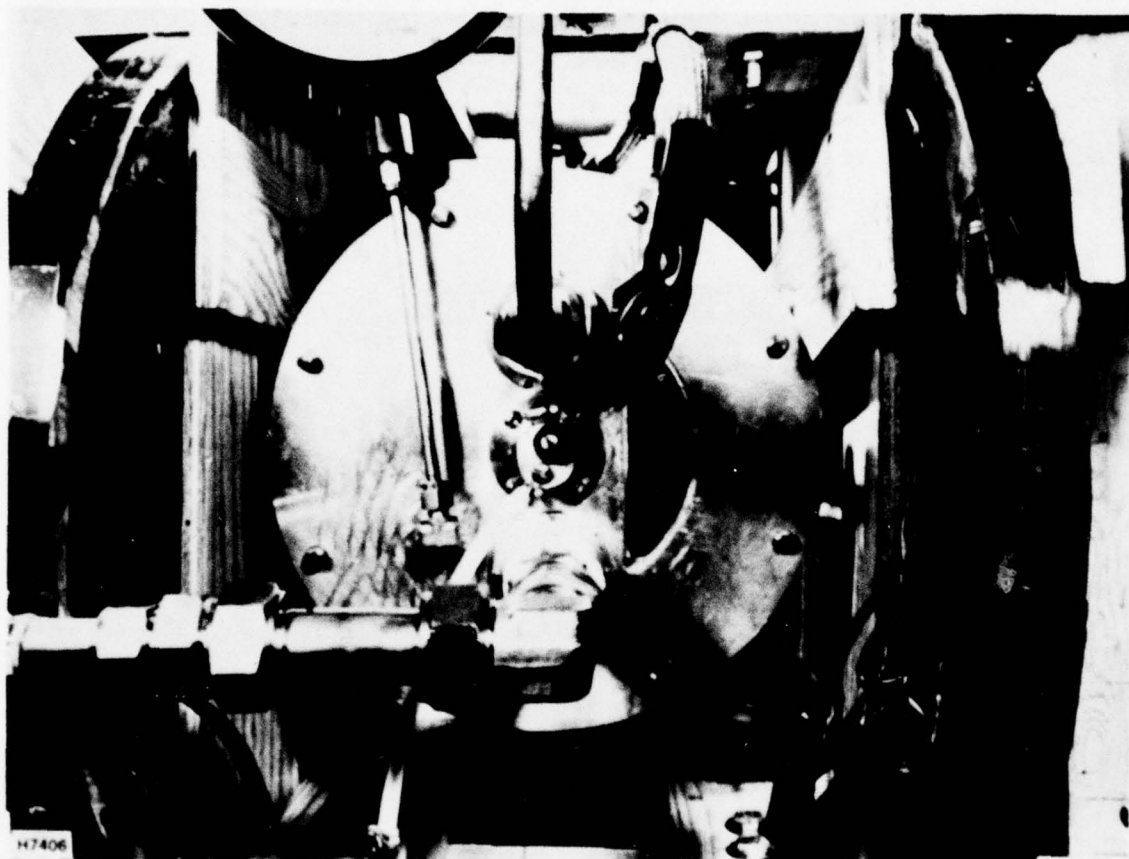
Figure 7c   A Camera-Eye View of the New Discharge Cell
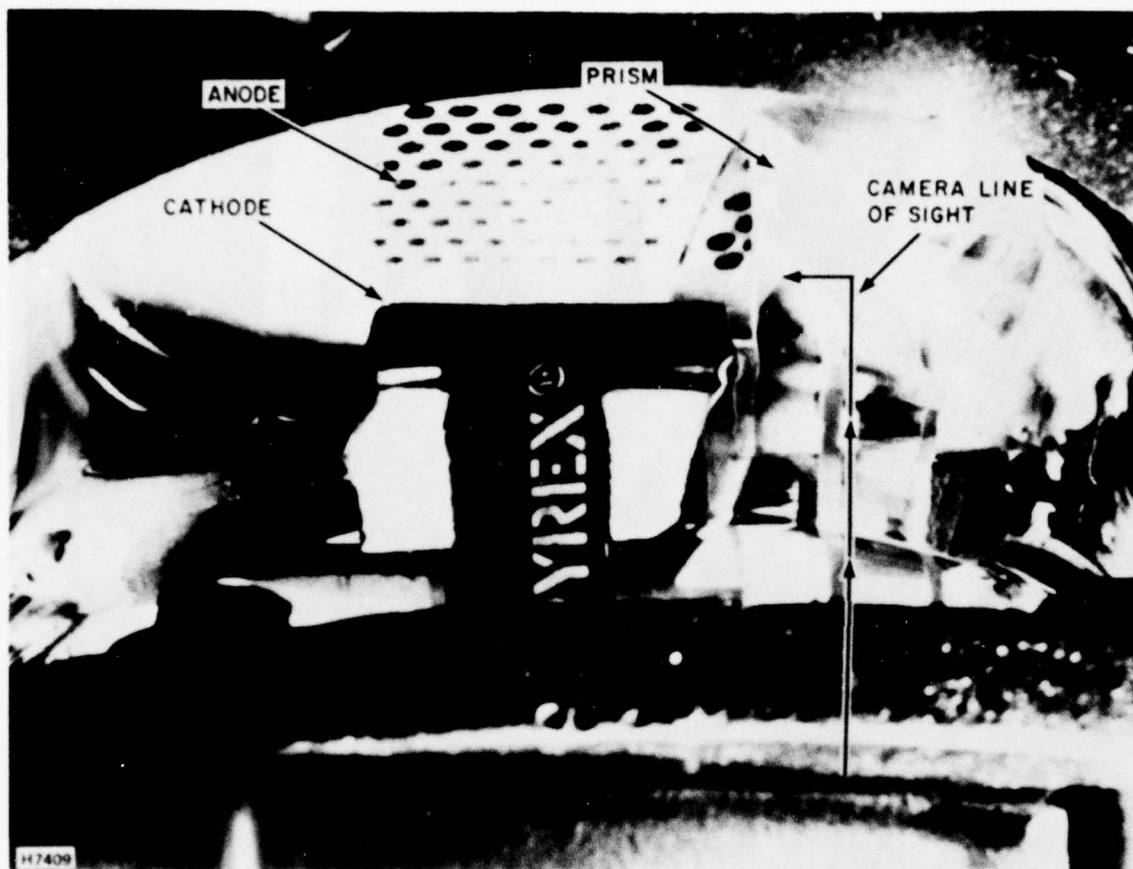
Figure 7d   A Close-Up View of the New Discharge Cell

FILM 1   760 TORR N$_2$ 4.0 KV/CM
0.72 mA/CM^2 E-BEAM   NO MAGNETIC FIELD

INCREASING TIME

ONE FRAME

ARC

H7399
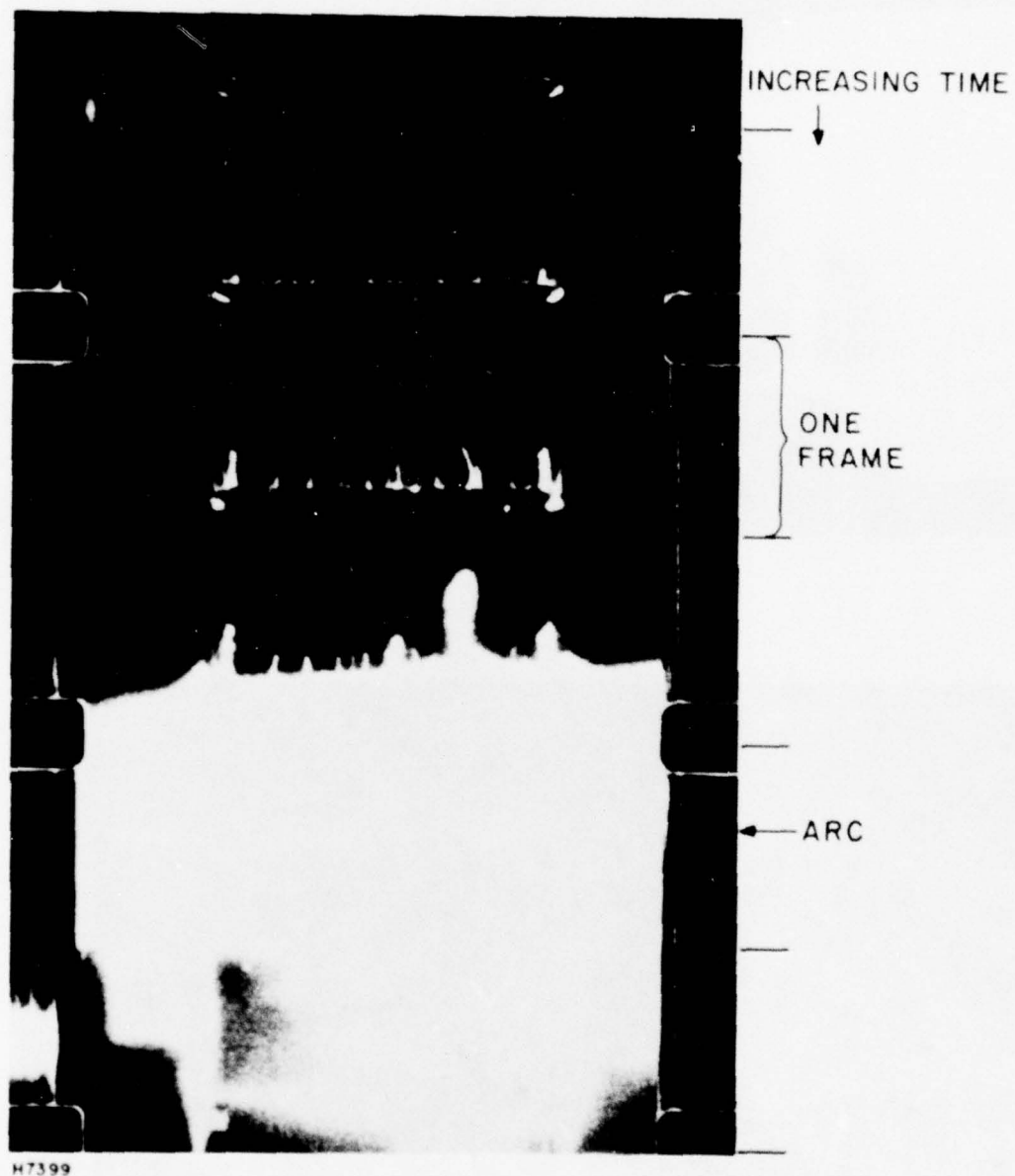
Figure 8   Streamer Growth

15

FILM 5 CONTINUED

H7400
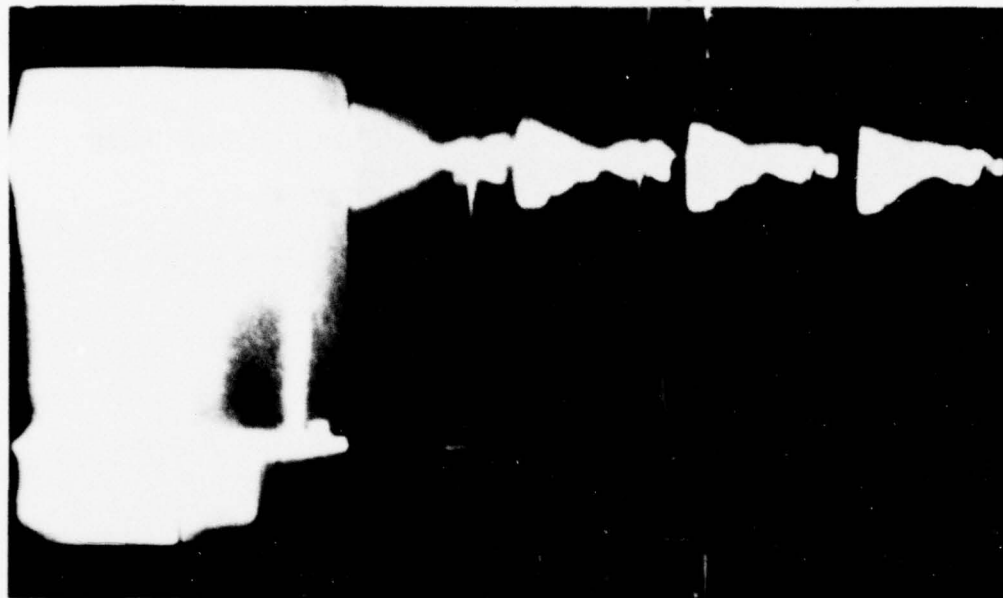
FILM 5   760 TORR N₂   3.7 KV/CM

0.72 mA/CM² E-BEAM   NO MAGNETIC FIELD

H7401
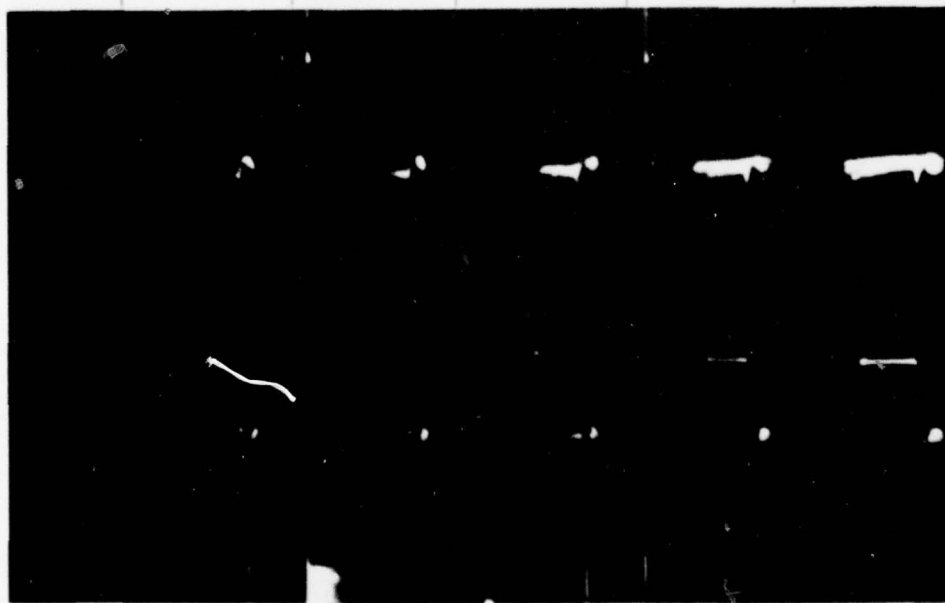
Figure 9   Streamer Growth

16

FILM 6   760 TORR N_2 3.7 KV/CM
0.72 mA/CM² E-BEAM   150 GAUSS MAGNETIC FIELD
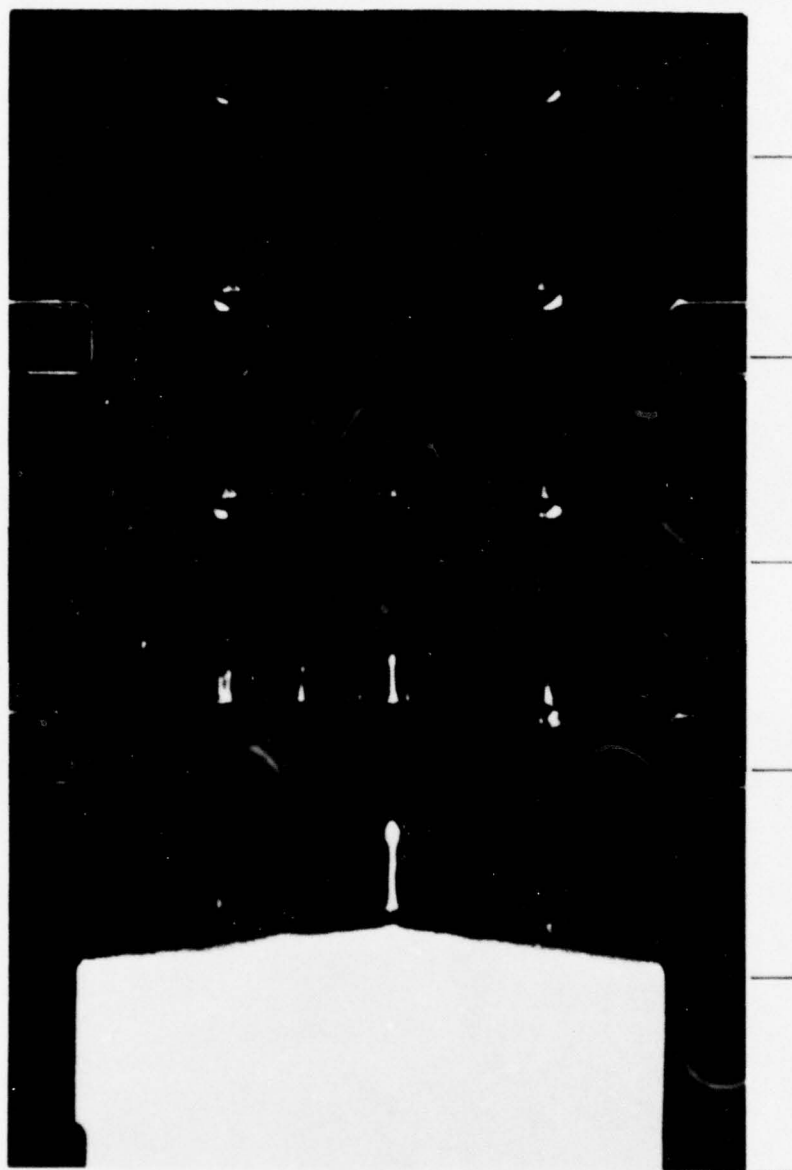
H7390

Figure 10   Streamer Growth

FILM 9   760 TORR N₂   3.3 KV/CM
0.72 mA/CM² E-BEAM   150 GAUSS MAGNETIC FIELD
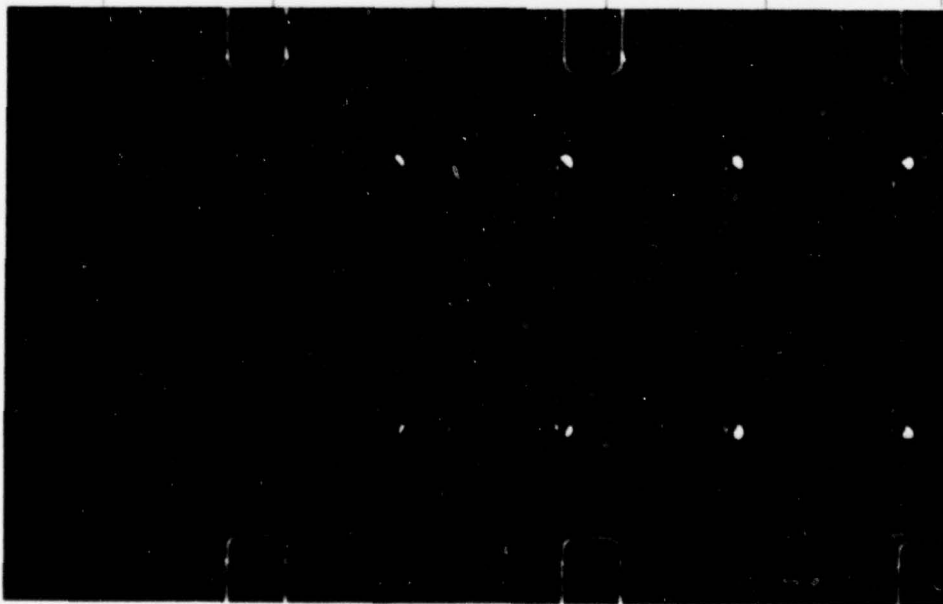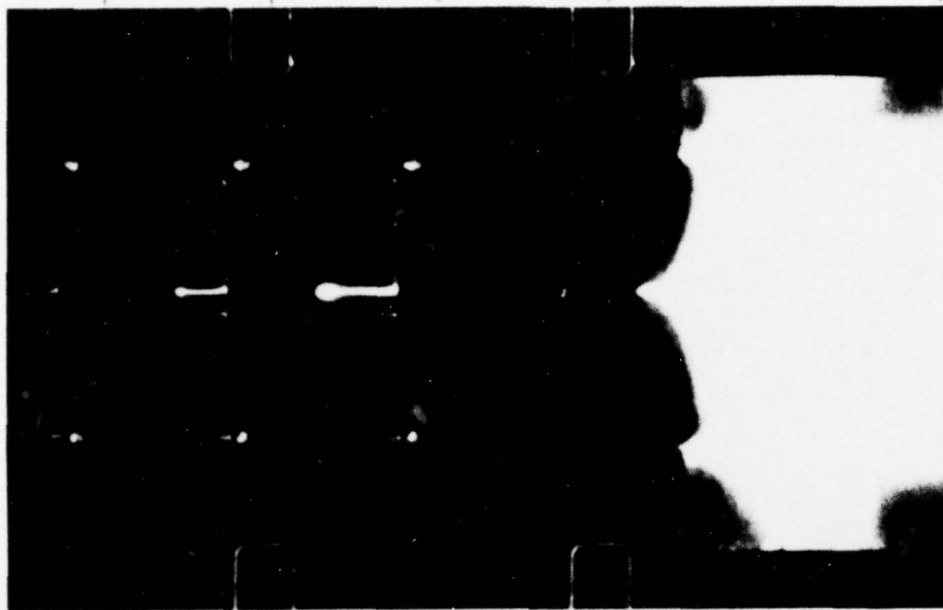
FILM 9   CONTINUED

Figure 11   Streamer Growth

FILM 14   500 TORR N₂   2.6 KV/CM

0.72 mA/CM² E-BEAM   NO MAGNETIC FIELD
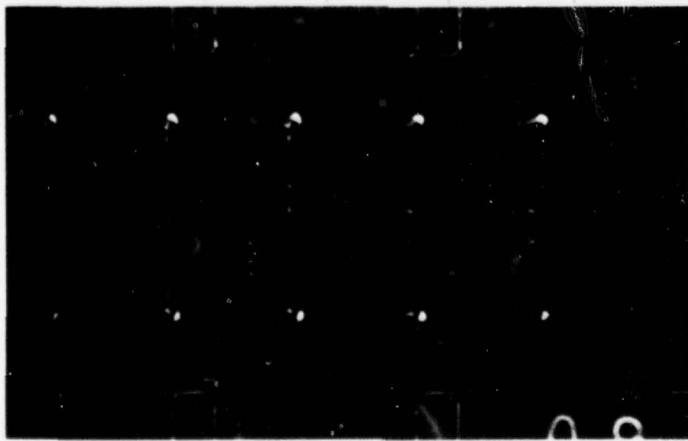
FILM 14   CONTINUED   (16 FRAMES OMITTED)

FILM 14   CONTINUED   (THIRD SECTION)
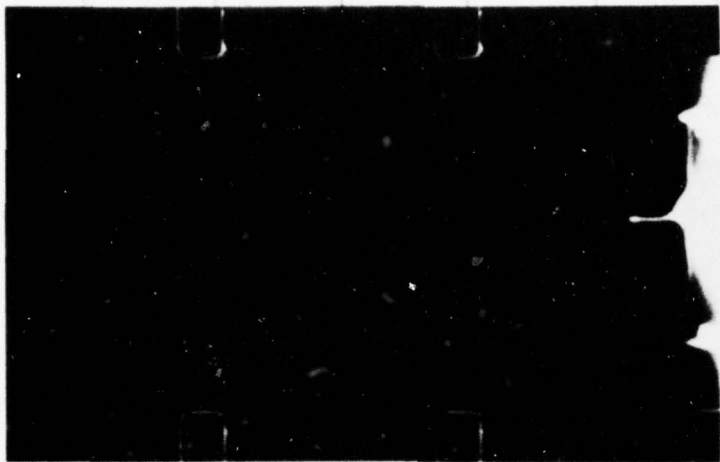
Figure 12   Streamer Growth

19

FILM 16   500 TORR N_2 29 KV/CM

0.72 mA/CM^2 E-BEAM   168 GAUSS MAGNETIC FIELD

H7396
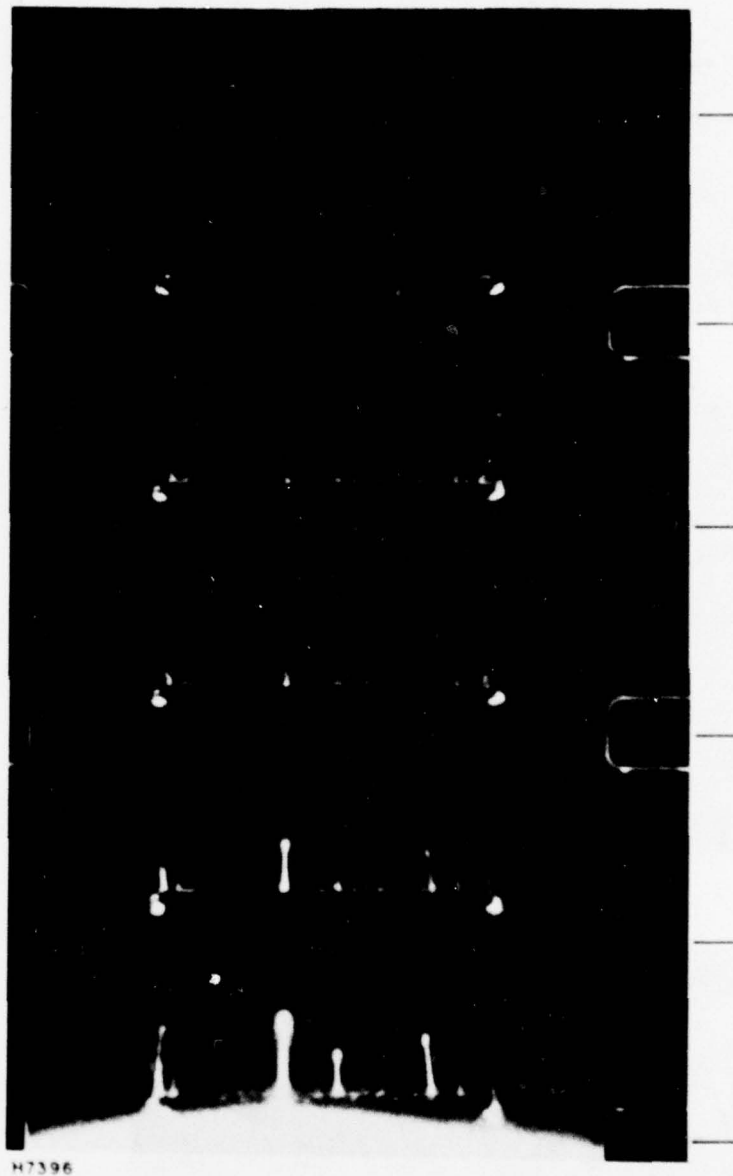
Figure 13   Streamer Growth

20

For each such shot, oscilloscope traces of the discharge voltage and the discharge, e-beam, and magnet coil currents were recorded, as well as the composition and pressure of the fill gas, the e-beam current setting, and the charging voltages of the sustainer, e-beam, and magnet coil banks. We thus have a quite detailed description of each shot, as shown in Table 1 which lists the data for the shot shown in the photo sequence in Figure 13.

Figure 8 shows a typical discharge which produced an arc 155 μs after the beginning of the pulse. Many streamers can be seen and the last frame clearly shows which one produced the arc. Figure 9 shows a similar shot at a slightly lower voltage. Here the time to arc was longer (265 μs), so the streamer growth can be seen in more detail. A whole row of streamers is evident growing from one edge of the cathode. It is interesting to note the bright spots at the edges of the cathode. These are grooves in the side of the cathode plate (see Figure 14) which appear to be acting as hollow cathodes.

Figure 10 shows a discharge under conditions identical to Figure 9 except for the addition of an external magnetic field. The B-field had no clear effect on streamer growth, and no sideways motion of the streamer is apparent. But note that this discharge arced in the center, while in Figure 9 the arc is at the edge. This is a surprising, but reproducible result. On all six runs we took with an imposed B-field, the arc was in the center. In ten runs in nitrogen without a B-field, the discharge usually (seven times) arced at the edge. It should be noted that an arc which appears to be in the center might be on the front or back edge; but in Figure 11, which shows the cathode after completion of these experiments, one can see burn marks where the arcs occurred, and some are in the center. Indeed, there are two groups of burn marks, one set along the edges and another set clumped in the center, with only a few intermediate cases. Evidently, this distribution is related to the streamer initiation process which we plan to explore further in subsequent work.

Figure 11 shows another new observation: a filmed record of a post arc. In this shot, the e-beam shut off before the streamer had reached the anode and the discharge current dropped almost to zero. But the streamer continued to grow and produced an arc roughly 100 μs later. Figure 12 shows an even more pronounced example. This arc did not occur until about a millisecond after the discharge, but, as can be seen, it was still caused by formation of a streamer. These films are our first direct evidence that streamers are responsible for post arcs.

Figure 13 shows a discharge in which several streamers grew to significant lengths before the strongest one produced

21

TABLE 1

DATA FROM RUN 9, OCT. 19, 1978 (Film 16)

Pressure and gas: 500 torr N_2
Sustainer bank voltage: 8 kV
e-beam current: 0.28 A, 0.67 mA/cm^2
e-beam voltage: 90 kV unattenuated, approx. 75 kV after foil
Coil bank voltage: 1.0 kV
Magnetic field: 166 gauss
Apparent location of arc: center
e-beam pulse duration: 220 μs
Time to arc: 227 μs
Streamer exponentiation Time: 86 μs
e-foldings to arc: >2.56, <2.64

	Initial	Final
Sustainer voltage (kV)	7.66	5.66
Electric field (kV/cm)	3.01	2.23
Sustainer current (A)	36.0	32.0
Current density (A/cm^2)	1.44	1.28
Power deposition (kW/cm^3)	4.34	2.85
Discharge resistivity (kΩ-cm)	2.09	1.74
E/N (kV/cm-atm)	4.58	3.39
Energy deposition (J cm^{-3})		.81

Comments: At least seven sizable streamers are visible. In the
early frames those near the edge are larger, but are
later overtaken by a brighter streamer near the center.
The last frames also show a second streamer near the
center which is relatively bright for its size and
appears to be growing rapidly.
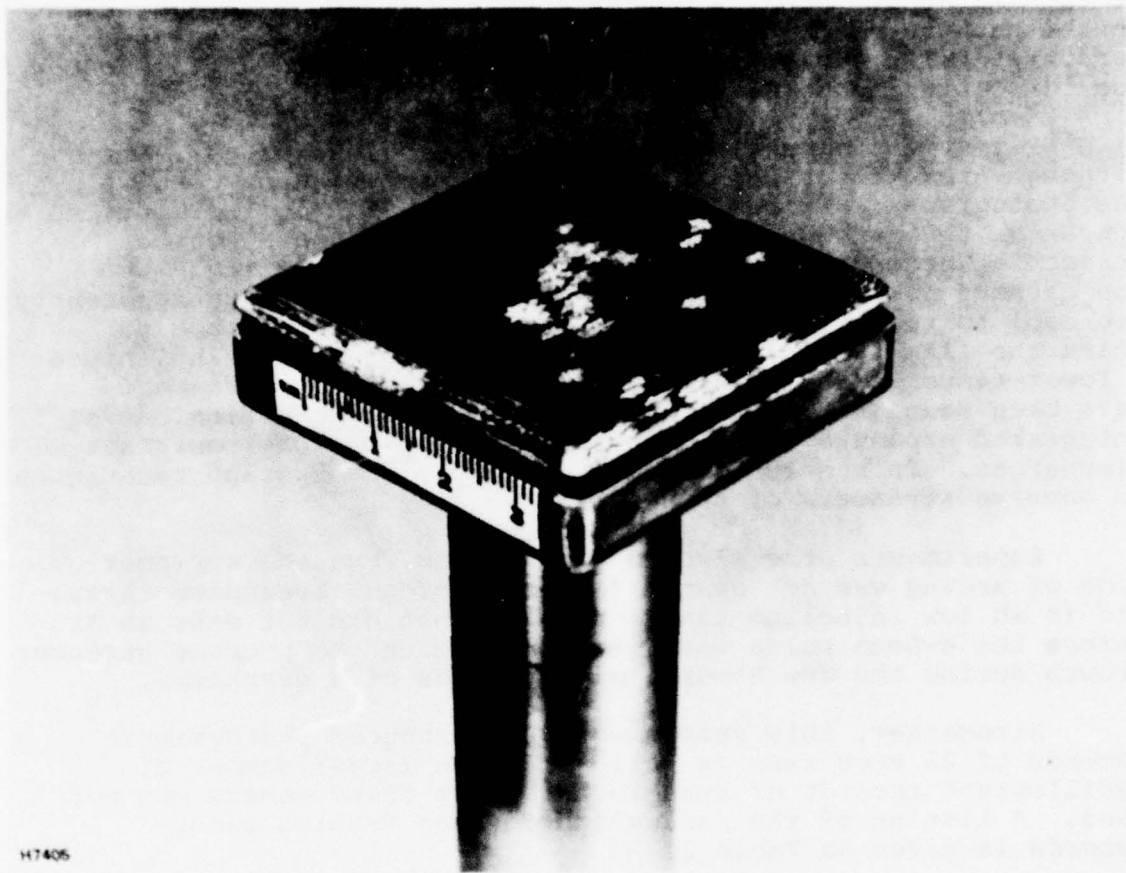
Figure 14   A View of the Cathode After the Experiments, Showing
Burn Marks

an arc. Here, as in some of the other films, one can see streamers bending toward the center of the discharge. It is not clear if this is due to bending of the electric field or to a gradient in the background conductivity, current density, and gas temperature. (The e-beam is nonuniform, being peaked at the center due to scattering on passage through the foil.)

Films were also taken of shots in 3:2:1 laser gas, but although these discharges did arc, streamers are not seen in the photographs. As can be seen in Figure 15, glowing spots do appear on the cathode early in the discharge, and a conical structure, presumably the base of a streamer, is visible on the cathode just before the arc, but the streamers are apparently too cool to radiate sufficiently in the wavelength range to which the film is sensitive. This is not too surprising, since a lower temperature is sufficient to ionize CO_2. Streamers have been seen in 3:2:1 gas in other discharge cavities, using integrated exposure techniques and exposing the gas resistant discharges. In the future, we hope to use shadowgraph techniques to observe streamers of this sort.

Experiments were also done in helium, but the streamer mode of arcing was not seen. The conventional breakdown threshold is so low in helium that a voltage that did not make an arc before the e-beam pulse was also insufficient to produce streamer growth during the few hundred microseconds of a discharge.

Altogether, this year's work has produced photographic records of 25 such runs as well as a much larger number of oscillograph records of runs in which the frame camera was not used. A listing of the runs which do have framing camera records is given in Table 2.

The new data on nitrogen, which now includes discharges at low pressures, are consistent with our earlier results. We find that streamer growth is exponential, except in the early stages when the streamer is less than a few millimeters long. In that initial stage, which was not seen last year because of the use of the loop of tungsten wire, the growth appears to be faster than the exponentiation seen later. We also find less correlation now between the time to arc and the observed growth rate of a developed streamer. There is some variability in the time required to initiate a streamer, an observation which gives cause for optimism that a proper choice of cathode can reduce the frequency for arcing in such discharges. In the later stages of growth, we observe an exponentiation time with parametric scaling like that seen before, provided that the electric field and the power density are both scaled to the pressure of the gas.

24

FILM 21   760 TORR 3-2-1   4.8 KV/CM

0.132 mA/CM^2 E-BEAM   NO MAGNETIC FIELD
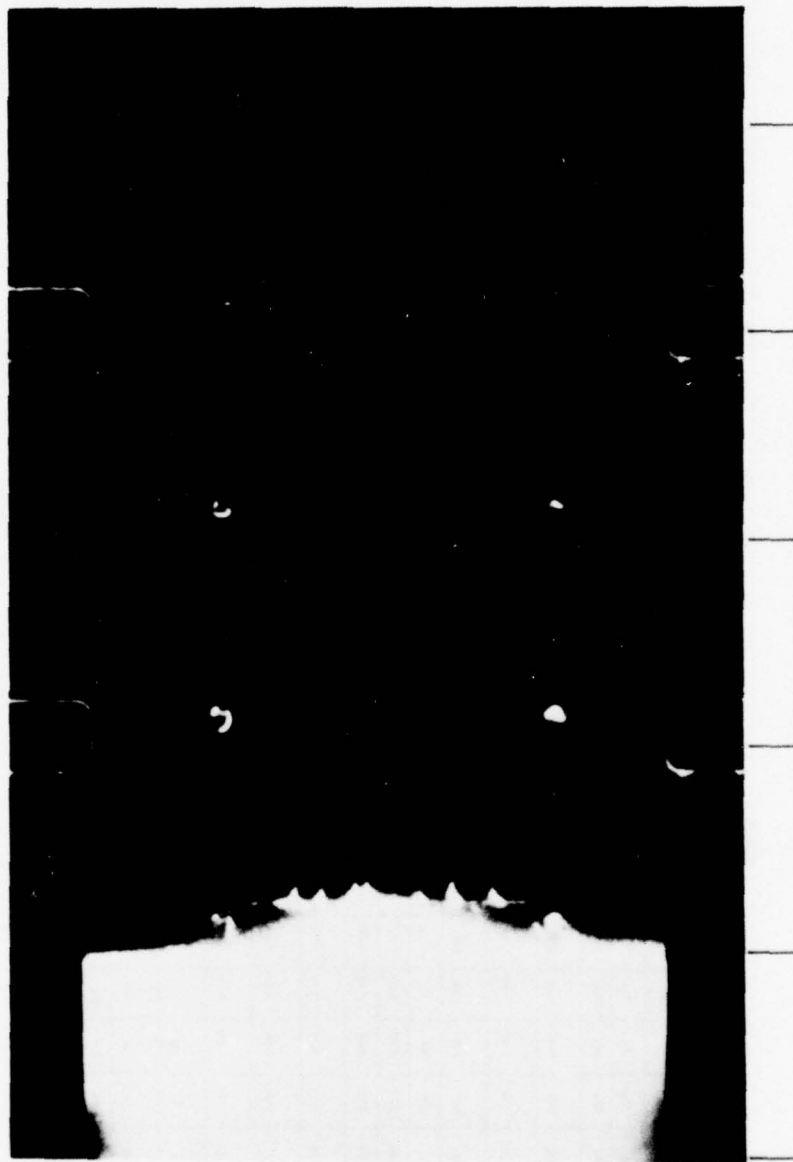
H7397

Figure 15   A Discharge in 3:2:1 Laser Gas

25

TABLE 2. DISCHARGES PHOTOGRAPHED WITH THE FRAMING CAMERA, OCT. 1978

DATE	10/17							10/19																		
RUN	2	3	4	5	6	7	8	1	2	3	4	5	6	7	8	9	10	11	12	13	14	15	16	17	18	
FILM	1	2	3	4	5	6	7	8	9	10	11	12	13	14	15	16	17	18	19	20	21	22	23	24	25	
GAS	N_2	N_2	N_2	N_2	N_2	N_2	N_2	N_2	N_2	N_2	N_2	N_2	N_2	N_2	N_2	N_2	3–2–1	3–2–1	3–2–1	3–2–1	3–2–1	3–2–1	N_2	N_2	N_2	
PRESSURE (torr)	760	760	760	760	760	760	760	760	760	760	760	760	760	500	500	500	760	760	760	760	760	760	500	300	300	
SUSTAINER BANK VOLTAGE (kV)	11.0	11.0	11.0	11.0	10.0	10.0	10.0	9.0	8.0	8.0	12.0	12.0	11.0	7.0	8.0	8.0	10.0	8.0	11.0	10.0	13.0	13.0	10.0	6.0	7.0	
E-BEAM CURRENT DENSITY (mA/cm^2)	.72	.67	.48	.67	.67	.72	.56	.79	.72	.56	.14	.10	.14	–	.62	.67	.66	.60	.14	.65	–	.12	.12	.13	.14	
E-BEAM PULSE DURATION (μs)	200	200	202	198	285	285	285	285	285	285	283	285	333	202	225	220	224	252	252	254	252	251	250	256	252	
B-FIELD (GAUSS)	0	125	240	0	0	150	216	0	154	0	0	180	0	0	0	168	0	0	0	146	0	0	0	0	0	
INITIAL E/N (kV/cm-atm)	4.45	3.75	4.02	4.04	3.51	3.84	3.80	2.91	3.33	2.91	4.47	4.52	4.04	3.80	4.48	4.58	3.90	3.13	4.14	3.73	–	5.00	5.73	5.47	6.41	
FINAL E/N (kV/cm-atm)	3.51	3.19	3.56	3.00	2.40	3.08	3.05	1.92	2.46	2.04	3.83	4.11	3.32	2.66	3.02	3.39	3.22	2.43	3.77	3.22	–	4.72	5.00	4.33	5.73	
INITIAL RESISTIVITY (Ohm-cm)	2.34	3.13	4.19	2.13	1.95	2.59	3.75	2.24	2.56	2.08	5.45	10.8	5.05	1.88	1.68	2.09	2.48	2.71	8.29	4.66	–	10.0	5.24	3.86	3.86	
FINAL RESISTIVITY (Ohm-cm)	1.67	2.45	5.09	1.39	1.25	2.20	4.77	1.39	2.46	1.85	3.83	10.3	3.32	1.33	1.21	1.74	1.84	1.84	4.71	2.68	–	5.58	3.42	2.38	2.83	
ENERGY DEPOSITION JOULES/cm^3)	1.23	.79	1.28	1.39	1.45	1.19	.77	.84	.97	.90	.93	.50	.99	.61	.95	.79	.95	.78	.59	.69	–	.50	.50	.31	.28	
APPARENT ARC LOCATION (CENTER OR EDGE)	C	C	C	E	E	C	C	C	C	C	E	C	E	C	C	C	C	C	C	C	C	C	E	E	E	
STREAMER EXPONENTIATION TIME (μs)	56	48	94	85	109	67	107	78	102	180	96	88	103	–	80	86	–	–	–	–	–	–	64	96	44	
TIME TO ARC (μs)	156	182	>202	197	285	230	>285	260	>285	>285	247	285	303	>202	>225	>220	177	252	232	200	182	157	171	>256	165	
E-FOLDING TO ARC	2.77	3.79	–	2.32	2.43	3.43	–	3.33	–	–	2.74	3.24	2.84	–	>2.81	>2.56	–	–	–	–	–	–	2.67	>2.66	3.75	

H9649

SECTION III

THEORETICAL ANALYSIS AND COMPARISON WITH DATA

1. STREAMER MODEL

Our original model of a streamer, shown in Figure 3 above, included a core cylinder, essentially an arc, of length c and radius b, a cap sphere or halo of radius a, where the conductivity is high due to ionization by the field and current concentration around the tip of the streamer column, and finally the background discharge of cold gas with uniform conductivity produced by the e-beam. This model was postulated before we had any detailed data about streamer structure, but it has been well borne out by our subsequent experimental work. As is evident in the framing camera photographs in the preceding section, streamers quite consistently display the structure which we had predicted.

In previous work under this contract, the model was quantified in considerable detail and used to predict such parameters as the temperature and the diameter of the streamer column, the size of the luminous halo, and the rate of growth of the streamer under various discharge conditions. The predicted streamer growth rate is in partial agreement with our observations. The streamer velocity deduced from the model is certainly of the right order, which gives us confidence that the basic mechanism, resistive heating of the gas near the streamer tip, is correct. As reviewed below, the model predicts that the streamer growth rate should be primarily dependent on the power density in the background discharge. This is found to be true in some, but not all of the parametric regimes which have been studies in our e-beam discharge.

To improve the accuracy of the model we believe it necessary to describe in more detail the heating processes around the streamer tip. The tip is a complicated structure where the gas and electron densities and temperatures and the electric field strength and current density are all rapidly varying. Beyond the tip the conductivity is due to e-beam ionization of the gas. Within the halo we believe the conductivity is due to ionization by electron multiplication, because the field is near the critical field, and to thermal ionization since the gas is heated by the increased current. In the outer regions of the halo, heating leads to an expansion of the gas; towards the center of the halo heat conduction must become important as the hot gas becomes part of the arc-like central column of the streamer.

27

A detailed analysis must include all these interacting nonlinear processes in a consistent manner. We do not yet have such a description, but we have made substantial progress toward it. This year we have included in our model gas heating ahead of the streamers, near the edge of the halo, and within the halo, making it possible to estimate the relative importance of these different effects in the different regimes where the discharge can be operated. Moreover, we now have what we believe to be a more precise description of the radial variation of vapor density, electric field and conductivity within the halo, a region which we had previously been able to describe only phenomenologically. By assuming that the field within the halo is damped at the breakdown threshold, and combining this with an analysis of the vapor expansion due to heating, we have been able to derive scaling laws which put our earlier model on a firm foundation and suggest a way in which it should be possible in future work to construct from first principles a more complete description. In what follows, our earlier calculations are reviewed and then the more recent work is described. Since the earlier work was covered in last years's final report[5], we are including here only a brief summary of the essential points.

2. STREAMER CURRENT AND CORE RADIUS

Since the electrical conductivity is high within the streamer, the streamer current is determined by the resistivity of the background discharge. The streamer is essentially a resistively ballasted arc, with the cold, e-beam ionized gas ahead of the streamer imposing the limiting resistance. Since the e-beam generated conductivity is uniform, and the current is quasi-static (i.e., divergenceless) one has,

$$\nabla \cdot (\sigma_o \underline{E}) = \sigma_o \nabla \cdot \underline{E} = - \sigma_o \nabla^2 V = 0$$

So the potential obeys Laplace's equation and hence is conveniently described in spherical coordinates in terms of Legendre polynominals. Assuming that the streamer halo is a conducting sphere with uniform surface potential V_1, that the E-field far from the streamer is uniform and of magnitude E_O, and that the potential at the base of the streamer ($\theta = \pi$, $r = c$) is zero, one obtains a reasonably accurate description in terms of the first few Legendre polynomials:

$$V = E_o \left(r - \frac{a^3}{r^2}\right) \cos \theta$$
$$+ \frac{1}{1 - \frac{2}{c}} \left\{ E_o c \left(1 - \frac{a^3}{c^3}\right) - \frac{aV_1}{c} + \frac{a}{r} \left[V_1 - E_o c \left(1 - \frac{a^3}{c^3}\right)\right] \right\} \tag{2}$$

5. Electron-Beam Sustainer Discharge Streamers and Arcing," Final Technical Report (Nov. 1977).

where, again, c is length of the streamer column, and a is the radius of the halo or cap sphere. Since the conductivity of the streamer is much higher than that of the background gas, the potential V_1 of the halo surface must be close to zero. So at least as a first approximation (which is probably as accurate as our assumption that the halo is at uniform potential) one can set $V_1 = 0$. Then differentiating Eq. (2) to find the strength of the radial field at the edge of the halo gives,

$$E_{r=a} = E_o \left[(1 + \frac{c}{a} + \frac{a}{c}) + 3 \cos \theta \right] \tag{3}$$

From this equation one can determine the streamer current. Setting $j = \sigma_o E$ and integrating over the surface of the cap sphere gives the total current,

$$I = \int_0^\pi \sigma_o E_{r=a} \, 2\pi \, a^2 \sin \theta \, d\theta$$

$$= 4\pi \, a^2 \, \sigma_o \, E_o \left[\frac{7}{4} + \frac{c}{a} \right] \tag{4}$$

where the second term in Eq. (3) has been integrated over the upper hemisphere and a/c has been neglected because it is much smaller than c/a.

Our original model also used Laplace's equation to estimate the radius of the top of the streamer column, i.e., of the hot core inside the halo. Reasoning that while the conductivity is not exactly constant within the halo (it probably does not change too abruptly), one can estimate b, the core radius, by taking $V = 0$ at $r = b$ and expanding in Legendre polynomials as above. By then assuming that $E = E_o$ at $r = a$ one obtains an estimate of the ratio a/b,

$$\frac{a}{b} \approx \sqrt{\frac{c}{b \left(\frac{E_c}{E_o} - 1 \right)}} \tag{5}$$

3. TEMPERATURE OF THE STREAMER COLUMN

In the main column of the streamer, the electron temperature and density are in equilibrium with the neutral gas, so the degree of ionization obeys Saha's equation at the temperature of the neutral gas. The electric field is low, but the current density is high, so the resistive power input is sufficient to keep the column hot. In gas at atmospheric pressure with a temperature below 3×10^4 °K, heat loss is mainly by conduction.

Without knowing the details of the column structure one cannot solve the heat flow equation exactly, but following Raiser[6] we proceeded by averaging it over the column area. This gives,

$$\frac{I^2}{\pi b^2 \sigma} = \pi A \int_0^T \kappa \, dt' = \pi A \bar{\kappa} T \qquad (6)$$

where b is the column radius. T is the mean temperature of the gas within the column, κ is the thermal conductivity, and A is a numerical factor characteristic of the gas. For high temperature air, Raiser's value of A is 15, which we used for nitrogen in our model. The mean thermal conductivity,

$$\bar{\kappa} \equiv \frac{1}{T} \int_0^T \kappa(T') dT'$$

is derived from the published conductivity for air[7] at high temperatures. Over the range of interest, $1500°K < T < 1500°K$, $\bar{\kappa}$ can be approximated by the analytic expression,

$$\bar{\kappa} = \kappa_0 T^{1.893} = 3.145 \times 10^{-10} T^{1.893} \text{ W/cm}^2°K \qquad (7)$$

Under pressure balance, the gas density is inversely proportional to temperature, and the electrical conductivity scales directly with electron density and inversely with gas density, so

$$\sigma = \sigma_0 \left(\frac{T}{T_0}\right) \left(\frac{n_e(T) + n_{eo}}{n_e(T_0) + n_{eo}}\right) \simeq \sigma_0 \left(\frac{T}{T_0}\right) \left(1 + \frac{n_e(T)}{n_{eo}}\right) \qquad (8)$$

where σ_0, T_0 and n_{eo} are the conductivity, temperature, and e-beam generated secondary electron density of the background discharge. The electron density in the streamer column, $n_e(T)$ is described by the Saha equation.

$$n_e = \frac{L_0 T_0 P_0}{T} \frac{f}{2} \left[\sqrt{1 + \frac{4}{f}} - 1\right] \qquad (9)$$

where

$$f = 2 \frac{u_1}{u_0} \frac{1}{T_0 L_0 \beta} \left(\frac{2\pi n_e k}{\kappa^2}\right)^{3/2} T^{5/2} e^{-I/kt}$$

and L_0 is Loschmidt's number, P_0 is the pressure in atmospheres, u_1 and u_0 are the statistical weights of the ion and atom. β is the degree of dissociation of a molecular gas ($\beta=2$ for nitrogen in the regime of interest) m_e, k, and h are the electron mass,

6. Raiser, Y.P., Sov. Phys. JETP, 31, 1148 (1970).

7. NACA, TN 4150 (1958).

Boltzmann constant, and Planck constant, respectively, and I is the ionization potential [8].

Combining Eqs. (4) through (8) one obtains,

$$T^{3.893} \left(1 + \frac{n_e(T)}{n_{eo}} \right) =$$

$$= \frac{16 \, T_o \, \sigma_o \, E_o^2 \, c^2}{15 \, \kappa_o \left(\frac{E_c}{E_o} - 1 \right)^2} \left[\frac{7}{4} + \sqrt{\frac{c}{d} \left(\frac{E_c}{E_o} - 1 \right)} \right]^2$$

Together with Eq. (9) for $n_e(T)$ this result gives the temperature T of a thermally stable streamer column. The result does depend upon b, but only very weakly. For a typical discharge in nitrogen (c = 1cm, b = 1mm, T_O = 300°K, σ_O = 2.6 x 10^{-4} mho/cm, E_O = 5000 V/cm). These equations predict that T = 6200°K. While some of the equations used in this calculation are merely rough estimates, the variation of electron density with temperature is so strong that temperature predicted by this calculation should be reasonably accurate.

4. REQUIRED ENERGY INPUT

We have hypothesized the streamer growth mechanism to be resistive heating by the concentrated current flowing into the streamer, its temperature rises toward that of the streamer column, making it part of the streamer, and causing the current concentration to extend farther into the background discharge. To analyze this process, one must know the energy required to heat the gas to the column temperature predicted by the calculation described in the preceding section.

In the subsonic regime, the energy required to raise one gram of gas at constant pressure from temperature T_O to T is equal to the enthalpy difference between these temperatures. Writing enthalpy as q(T), the energy is ΔQ = q(T) - q(T_O) joules per gram. The energy required to raise unit volume of gas over the same temperature range at constant pressure will then be,

$$\varepsilon = \int_{T_o}^{T} \rho \, \left(\frac{\partial q}{\partial T'} \right) dT'$$

---

8. Zeldovich, Y.B., and Raizer, Y.P., Physics of Shock Waves and High Temperature Hydrodynamic Phenomena, A.P. New York (1966).

where $\rho = \rho(T')$ is the density of the gas. Since $\rho = \rho_O T_O/T$, where ρ_O is the density at T_O, this reduces to

$$\varepsilon = \rho_O \, T_O \int_{T_O}^{T} \left(\frac{\partial q}{\partial T'}\right) \frac{dT'}{T'}$$

Physically, as a constant volume of gas is heated under constant pressure, the gas expands and some leaves the volume, removing energy, but leaving less gas in the volume to be heated further. The above expression for ε, the "constant volume constant pressure enthalpy" includes these effects.

For molecular gases. $\varepsilon(T)$ can be quite complicated, but over a limited range of temperature it can usually be approximated by a simple power law. For nitrogen in the region of interest to us, data available in the thermodynamic tables[9] is adequately fitted by the simple formula,

$$\varepsilon = \varepsilon_O \, P_O \left(\frac{T}{T_1}\right)^{0.63}$$

where $\varepsilon_O = 1.0$ J/cm^3. $T_1 = 3500°K$, P_O is the pressure in atmospheres, and ε is the energy required to heat 1 cm^3 of gas from $300°K$ to T. For the streamer column temperature calculated above, $T = 6200°K$, this gives a needed input energy of $\varepsilon = 1.4$ J/cm^3.

5. HEATING AT THE HALO EDGE

In our original model, we calculated the resistive heating within the halo under the assumption that the conductivity varied radially as

$$\sigma = \sigma_O \, e^{k\left(\frac{a}{r} - 1\right)}$$

This form was simply postulated, but the heating rate it gives should be a reasonable estimate if the conductivity does increase rapidly as one moves into the halo. (In support of this we considered alternate forms and showed that the result was practically unchanged.) Using this expression one can integrate j^2/σ over the cap sphere from the edge of the core to the edge of the halo to obtain,

$$Q = \int_{b}^{a} \frac{I^2}{(4\pi \, r^2)^2} \frac{4\pi \, r^2}{\sigma_O} e^{k\left(1 - \frac{a}{r}\right)} dr$$

$$= \frac{I^2}{4\pi \, \sigma_O \, ak} \left[1 - e^{-k\left(\frac{a}{b} - 1\right)}\right] \text{ watts.}$$

---

9. Lewis, C.H. and Burgess, E.G., "Tables of Thermodynamic Properties of Nitrogen from 1500 to 15000°K; T.N. AEDC-TDR-63-138 (1963).

Since the ratio of conductivities in the core at 6200°K and in the background gas under e-beam ionization is apprimately 10^3 and $a/b \approx 3$, the value of k which matches the boundary condition on the conductivity is k = 3.45. Thus, the second term in the above equation is completely negligible and the mean power density within the halo is

$$\dot{q} = \frac{3I^2}{16\pi^2 \sigma_o a^4 k} \quad W/cm^3$$

From this power density one could compute the time required to heat the halo to the temperature of the core of the streamer. However, a heating time calculated in this way could be too long because only the center need be heated for the core to grow. In a calculation given in detail in the previous annual report we deduced a correction factor of $\lambda = 0.3$, which accounts for a radial temperature variation consistent with the above stated radial dependence of the conductivity.

From these results one can deduce a characteristic velocity for propagation of the streamer. It is the radius of the sphere a, divided by the time required to heat the gas in the halo interior to the core temperature, $\tau = \lambda\epsilon/\dot{q}$. Thus we have,

$$v = \frac{dc}{dt} = \frac{a\dot{q}}{\lambda\epsilon} = \frac{3I^2}{16\pi^2 \sigma_o \lambda a^3 k\epsilon}$$

$$= \frac{3a \sigma_o E_o^2}{\lambda k \epsilon} \left(\frac{7}{4} + \frac{c}{a}\right)^2$$

where we have used Eq. (4) to express the current I in terms of the other variables.

The model predicts that c/a should remain roughly constant as the streamer grows and this is confirmed by the framing camera photographs. Putting the result in a form more appropriate for such a scaling, and using the above derived values of λ, k, and ϵ, we have

$$\frac{dc}{dt} = \gamma c$$

where

$$\gamma = 2.07 \left(\frac{\sigma_o E_o^2}{P_o}\right) (\frac{a}{c}) \ (\frac{7}{4} + \frac{c}{a})^2$$

33

Hence the model predicts that streamers should grow exponentially. This prediction is in good agreement with our observations. The predicted growth rate, γ is primarily dependent upon the specific power loading, $\sigma_O E_O^2/P_O$. This is also in good agreement with the data over a considerable range of parameters. As can be seen from Figure 5, the line of constant growth rate is nearly a line of constant power density in the strong field regime. Since the assumptions underlying our theory (e.g., that the halo around the streamer tip extends well beyond the radius of the streamer column) are appropriate to the strong field operating mode, one expects agreement with experiment there. In the high current, low field regime, the resistive heating of the gas beyond the halo may be important and that heating was not included in the original model. We have done some analysis of heating ahead of the halo, as described in the next section, but in the regime of principal interest for laser applications, our original model is in good agreement with the data.

6. HEATING AHEAD OF THE STREAMER

The assumed variation of conductivity within the halo restricted our original model to effects of heating just inside the halo edge. Clearly, a more detailed theory should include a calculation of the power input throughout the vicinity of the growing streamer. We have now made considerable progress toward the development of a more complete description.

There is some heating beyond the halo, which can be estimated from the analysis already done. Just outside the halo the electric field is E_C, the critical field and the conductivity is σ_O. Therefore, the power input is $\sigma_O E_C^2$, which will heat the gas to the conductive temperature in a time $\tau = \varepsilon/\sigma_O E_C^2$. Since the scale length of this field is a, the halo radius, such heating alone would give a velocity $v = a/\tau$. We have not yet directly estimated a, but it is implied by Eq. (3) for the E-field beyond the halo. Setting $\theta = 90°$, and $E = E_C$ we have

$$E_C = E_O \left(1 + \frac{c}{a} + \frac{a}{c}\right)$$

or

$$\frac{c}{a} \approx \frac{E_C}{E_O} - 1$$

This is approximate, because the θ dependence has been omitted, but is consistent with our original approximation of the halo as a sphere (which was used to derive Eq. (2)). From this we have the propagation speed

$$v = \frac{dc}{dt} = \frac{c \, \sigma_O E_C^2}{\left(\frac{E_C}{E_O} - 1\right) 1.4 \, P_O}$$

34

or

$$\frac{dc}{dt} = \gamma \, c$$

where

$$\gamma = \frac{\sigma_o \, E_o \, E_c}{\left(1 - \frac{E_o}{E_o}\right) 1.4 \, P_o}$$

This is primarily dependent upon $\sigma_o \, E_o = j_o$, the current density within the background discharge. This is an extreme conclusion, since it ignores all heating within the halo, but we note that at low electric fields where heating beyond the halo becomes more important, the data in Figure 5 are not inconsistent with a constant growth rate line being a line of constant current density in the weak field, high current regime.

7. THE STRUCTURE OF THE HALO

We believe we have now found a way to describe the whole region around the streamer tip in more detail. Our new approach starts with the assumption that inside the halo, but outside the core cylinder, the electric field strength is clamped at the breakdown threshold level. We reason that the current is limited by the background discharge and hence cannot increase, so the E-field must be consistent with this current. If the E-field dropped below E_c, the conductivity would drop causing the field strength to increase again. But if the field rose much above E_c, the conductivity would be rapidly increased by electron multiplication, which would reduce the electric field toward E_c. We thus conclude that in the halo the field strength cannot be very different from the breakdown field.

However, this does not mean that the field strength is constant in the halo, because the breakdown field depends upon the gas density, which decreases as the gas is heated. More precisely,

$$E = \frac{nE_{co}}{n_o}$$

where by E_{co} is meant the breakdown field is the background discharge.

Within the halo one expects the current and the E field to be nearly radial, since both are diverging from the tip of the streamer column. This implies that the magnitude of the current density scales as

$$j \, \alpha \, \frac{1}{r^2}$$

35

Hence the power density must scale as

$$P = j.E \propto \frac{nE_{co}}{n_o r^2}$$

Matching this to the boundary condition at the halo edge gives

$$P = \sigma_o E_{co}^2 \; \frac{n}{n_o} \; (\frac{a}{r})^2$$

For nitrogen, it was demonstrated earlier that

$$\epsilon = \epsilon_o \; (\frac{T}{T_1})^{0.63}$$

Differentiating this, we have

$$j.E \; dt = d\epsilon = \frac{0.63 \; \epsilon_o}{T_1} \; (\frac{T}{T_1})^{-0.37} \; dt$$

We also know that $n = n_o T_o/T$, so

$$dt = - \frac{n_o T_o}{n^2} \; dn$$

Combining these results gives

$$\sigma_o E_{co}^2 \; (\frac{a}{r})^2 = \frac{0.63}{T_1} \; (\frac{T}{T_1})^{-0.37} \frac{n_o^2 T_o}{n^3} \; \frac{dn}{dt}$$

Now make the substitution $dn/dt = v \; dn/dr$ to obtain

$$n^{-2.63} \; \frac{dn}{dr} = \frac{K}{r^2}$$

where

$$K \equiv \frac{T_1^{0.63} \; \sigma_o E_{co}^2 \; a^2}{0.63 \; n_o^2 \; T_o \; v}$$

This has the solution, for $n = n_o$ at $r = a$,

$$n = \left[1.63 \; K \left(\frac{1}{r} - \frac{1}{a} \right) + \frac{1}{n_o^{1.63}} \right]^{-0.61}$$

36

Well inside the halo this reduces to

$$n = K' \, r^{0.61}$$

where

$$K' = (1.63 \, K)^{-0.61}$$

This result provides the scaling needed to develop a more comprehensive theory. That has not yet been done, but we note that the new result does provide a more solid foundation for our earlier model. From the above results we have that power density well inside the halo varies radially as

$$P \propto \frac{n}{n^2} \propto \frac{1}{r^{1.39}}$$

Since this increases with decreasing r, the power density is highest near the center of the halo, but since the increase is less rapid than $1/r^2$, most of the total power input to the halo is near the outer edge as we assumed. However, we now see that heating near the center is not negligible and must be included in a more complete description. (However, we have not yet included heat conduction, which will further reduce the power input near the core.)

Clearly, this last calculation is just the first step in the development of a second generation theory, but we think it is important because it shows how to proceed with that development.

8. MAGNETIC DEFLECTION OF THE STREAMER COLUMN

In the course of this year's experiments, a magnetic field was imposed transverse to the discharge to examine the possibility that this would push the streamers sideways through the cold background gas. No such effect was seen, although, as discussed above, the B-field did seem to affect the streamer location. The strongest field compatible with our e-beam was employed ~200 gauss, which gives a 100 kV electron a gyro radius of 5 cm, comparable to the dimensions of our e-beam. But a simple calculation shows that even this was marginal for the intended purpose. The current density in the background gas in our discharge is typically 1.5 amperes/cm^2. Since a well-developed streamer draws the current from about 1 cm^2 of discharge, we know that a typical streamer current is around 1.5 amperes. A magnetic field of 200 gauss would thus impose upon the streamer column a force of about 30 dynes/cm. A streamer column is a fraction of a millimeter in diameter, and the gas density is reduced by at least an order of magnitude from atmospheric density, so a reasonable estimate of the mass of the gas in the

column is 10^{-7} g/cm. If there were no resistance, the magnetic force would move this mass a millimeter or two in the few tens of microseconds available.

We would have observed such motion, but since there is resistance from the gas surrounding the column it is not surprising that the streamers did not move this far. Streamer motion sideways through the discharge is a complicated process, and there appears to be no simple way to predict exactly how much B-field is required. We thought there was a possibility of observing some small deflection in our apparatus, which would have given us a data point from which we could extrapolate, but this did not occur. Since stronger fields are not usable in our apparatus, this precludes further investigation of the process there.

However, there remains a distinct possibility that an external B-field would affect streamers in other discharge machines. One could apply a stronger B-field parallel to the e-beam. Indeed this is done in some large machines to minimize e-beam spreading. Since the sustainer discharge is normally parallel to the e-beam, such a field would not initially exert a force on streamers. But we know that in flowing gas systems, streamers are swept downstream, where they lead to downstream arcing. A streamer extending downstream would be transverse to the B-field, so there could be an effect. Moreover, the times involved are longer than in our machine, and the currents are larger, so our observations in no way preclude the possiblity of large deflections and resultant cooling of such streamers.

SECTION IV

CONCLUSIONS

In summary, extensive new framing camera data on streamer structure and development have well confirmed our model of a streamer as composed of core and halo surrounded by background discharge. Streamer growth is consistently seen to be exponential, with the ratio of length to halo radius remaining constant during growth for a wide range of discharge conditions. Our original theory predicts a growth rate primairly dependent upon power loading, and we find this to be true in the high field regime where laser discharges are operated, but not in the weak field, high current regime. The model has been further developed by calculation of heating ahead of the streamer and in the interior of the halo. Scaling laws for the density, temperature, and electric field distributions within the halo have been derived, and these provide a basis for the construction of a more complete theory in future work.

This year's work has established the need for a detailed mapping of the gas density and resistive power distributions around the tip of a streamer. We believe this can be done theoretically, and we have also proposed using shadowgraph techniques to obtain data on the density variation.

The imposition of a transverse magnetic field was not seen to affect the streamer growth rate or to move the streamer laterally, but practical limitations of our particular discharge prevented a complete examination of that question.

This year's work provided the first framing camera records of spontaneous streamer development from a smooth cathode surface. Considerable scatter is seen in the streamer formation times, indicating that more detailed study of the initiation process in the cathode layer would be valuable. This will also be pursued in future work.

REFERENCES

1. Douglas-Hamilton, D.H., Mani, S.A., J. Appl. Phys. 45, 4406 (1974).

2. AFOSR Final Report, Contract F44620-70-C-0023 (1974).

3. Jacob, J.H. and Mani, S.A., Appl. Phys. Lett. 26, 53 (1975).

4. Nighan, W.L. and Wiegand, W.J., Appl. Phys. Lett. 25, 633 (1974),

5. Electron-Beam Sustainer Discharge Streamers and Arcing," Final Technical Report (Nov. 1977).

6. Raiser, Y.P., Sov. Phys. JETP, 31, 1148 (1970).

7. NACA, TN 4150 (1958).

8. Zeldovich, Y.B. and Raizer, Y.P., Physics of Shock Waves and High Temperature Hydrodynamic Phenomena, A.P. New York (1966).

9. Lewis, C.H. and Burgess, E.G., "Tables of Thermodynamic Properties of Nitrogen from 1500 to 15000°K; T.N. AEDC-TDR-63-138 (1963).